Magnetostrictive stress reconfigurable thin film resonators for near direct current magnetoelectric sensors

Jillian Kiser, Ron Lacomb, Konrad Bussmann, Christopher J. Hawley, Jonathan E. Spanier, Xin Zhuang, Christophe Dolabdjian, Sam Lofland, Peter Finkel

Magnetostrictive stress reconfigurable thin film resonators for near direct current magnetoelectric sensors

Jillian Kiser,[1] Ron Lacomb,[1] Konrad Bussmann,[2] Christopher J. Hawley,[3] Jonathan E. Spanier,[3] Xin Zhuang,[4] Christophe Dolabdjian,[4] Sam Lofland,[5] and Peter Finkel[1,2,a)]

[1]*Naval Undersea Warfare Center, Newport, Rhode Island 02841, USA*
[2]*U.S. Naval Research Laboratory, Washington, DC 20375, USA*
[3]*Department of Materials Science and Engineering, Drexel University, Philadelphia, Pennsylvania 19104, USA*
[4]*Normandie Univ, France; UCBN, GREYC, F-14032 Caen, France; and CNRS, UMR 6072, F-14032 Caen, France*
[5]*Department of Physics, Rowan University, Glassboro, New Jersey 08028, USA*

(Received 7 January 2014; accepted 25 January 2014; published online 19 February 2014)

The magnetic response of microdevices is significantly enhanced at structural resonance allowing for improved sensitivity and signal-to-noise ratio. Here, free-standing thin film CoFe bridge resonators have been fabricated and investigated. It is shown that the strong magnetic field dependence of the fundamental resonance frequency is a function of magnetic field orientation due to stress-induced anisotropy. These devices may offer a new approach for developing fully integrated resonant magnetic field sensing technology. © *2014 AIP Publishing LLC*.
[http://dx.doi.org/10.1063/1.4866044]

Multiferroic magnetoelectric (ME) composites were introduced over a decade ago, making single phase ME materials obsolete in favor of the extraordinarily high magnetoelectric coupling of composite structures.[1] This high coupling makes the ME composite approach well suited for various applications including but not limited to electric field tunable electronic devices,[2–4] microwave magnetic devices,[5] energy harvesting,[6–8] and magnetic sensing.[9–13] In order to maximize performance as magnetic sensors, these devices must be optimized for high electronic signal output and low noise power in the frequency range of interest. Wang *et al.* demonstrated, for example, the macroscopic ME sensor with an equivalent magnetic noise floor of less than 5.1 pT/$\sqrt{\text{Hz}}$ at frequency $f = 1$ Hz[10] using excitation by the field itself. The important figure of merit, the signal-to-noise ratio (SNR), is enhanced by increasing the sensitivity of the sensor or by reducing the equivalent magnetic noise power. One promising method of increasing the sensitivity is in the development of ME sensors that operate at electromechanical resonance (EMR) where the ME coupling is typically several orders of magnitude higher than off-resonance operation.[3] Increasing the ME coupling coefficient, $\alpha_{ME} = dE/dH$, E and H being the electric and magnetic fields, respectively, ensures that even small changes in magnetic field result in significant electrical output, thereby increasing sensitivity. However, detection of quasi-static magnetic fields requires a relatively large sensor size for operation at EMR,[14] which is undesirable for many applications.

The alternative to achieving a low equivalent magnetic noise floor is to design a sensor which minimizes the noise power spectral density. This is particularly relevant for magnetic field sensing near dc and low ac frequencies where $1/f$ noise is prominent.[13] This noise can be minimized by operating at high resonance frequencies that, for MEMS implementations,[14,15] is commonly achieved by decreasing sensor dimensions.[16] Minimization also allows for ensemble averaging and noise reduction through wafer-scale fabricated device arrays with low cost. However, processing and fabrication of such devices retaining high magnetostriction and low loss yet present technological challenges, particularly in stress mitigation. One method of creating essentially stress-free FeCo for MEMS is described in Ref. 16. However, this method does not allow for synthesis of free-standing bridges with clamped ends to be used as stress reconfigurable magnetostrictive resonators, the approach potential for passive low frequency field detection.[17]

In this work we have fabricated and investigated mesoscopic scale thin film magnetoelastic sub-mm length ME fixed-fixed FeCo resonators. In the approach presented here, a shift of the fundamental bending mode frequency in these resonators was measured as a function of magnetic field and direction demonstrating high sensitivity at low frequency or near dc field. A process was developed to fabricate arrays of CoFe beams of various lengths L (500, 750, and 1000 μm) and constant width $w = 40$ μm and thickness $t = 500$ nm, which are free-standing and fixed at both ends to a silicon substrate (Fig. 1(a)). A 4-in double-sided polished n-Si wafer was coated with 3000 Å of Si_3N_4 at 800 °C by low-pressure chemical vapor deposition. The wafers were backside patterned with Shipley 1813 photoresist, and windows in Si_3N_4 were opened with reactive ion etching (RIE) with a mixture of CHF_3 and O_2. After stripping the photoresist, the windows were etched in heated (80 °C) 30% KOH to form membrane windows on the front side. Co and Fe were co-sputtered at room temperature from dual sources onto the Si_3N_4 windows. The CoFe was patterned with lift-off photolithography. The devices were annealed at 800 °C

a)Author to whom correspondence should be addressed. Electronic mail: peter.finkel@nrl.navy.mil

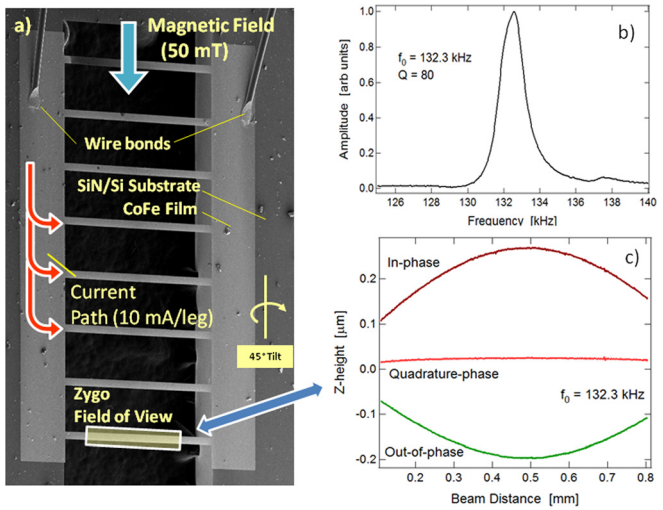

FIG. 1. (a) SEM image of selected beam array showing 40 μm $\times$ 1 mm beam set at 45° tilt; (b) Zygo beam resonance spectrum and (c) surface plot and linescan evaluation at named phase angles under Lorentz force excitation.

(following Ref. 15) for 1 h in a closed quartz ampoule evacuated to less than 1×10^{-7} Torr, with consequent water quenching after removal from the furnace. Then, the nitride was removed from the back side by RIE. Film composition was nominally $Co_{68}Fe_{32}$ as measured by energy dispersive spectroscopy.

The fundamental vibrational mode of the beam was determined by dynamic optical profilometry done with a Zygo NewView 7300 system equipped with dynamic imaging allowing for stroboscopic capture of beam deflection as a function of frequency, phase, and drive voltage. A substrate patterned with a 1-mm long $\times$ 40-μm wide beam array (7 elements) was mounted to a chip carrier and wires were bonded to opposite ends for electrical contact. The assembly was mounted within the objective field of view to image the central 0.7 mm of a selected beam (Fig. 1(a)). A lateral magnetic field ~50 mT was provided by SmCo magnets. An integrated function generator was used to produce ~10 mA through the selected beam, and the deflection resulting from the concomitant Lorentz force was imaged as a function of frequency. Figures 1(b) and 1(c) show the spectral response and the in-phase, out-of-phase, and quadrature phase profiles at the resonant frequency f_r of 132.3 kHz.

The magnetic field coupling to fundamental bending mode resonance was investigated by measuring the transverse beam deflection with laser Doppler vibrometry (LDV). In this method, a laser beam from the LDV (Polytec) with ~40-μm laser spot size was reflected off an individual bridge of a larger sample to detect the beam deflection. The beam was driven by a piezoelectric transducer with either a variable frequency source or with a 1-μs long square wave impulse. Impulse vibrometry data were recorded at a sample rate of 1.4 MHz for 0.5 ms and processed by fast Fourier transform (FFT) to determine the spectral content of the resulting motion, as shown in Fig. 2.

For another set of 1-mm bridges, it was found that the LDV results gave $f_r \sim 124$ kHz. The fundamental structural resonance frequency of a doubly supported beam is

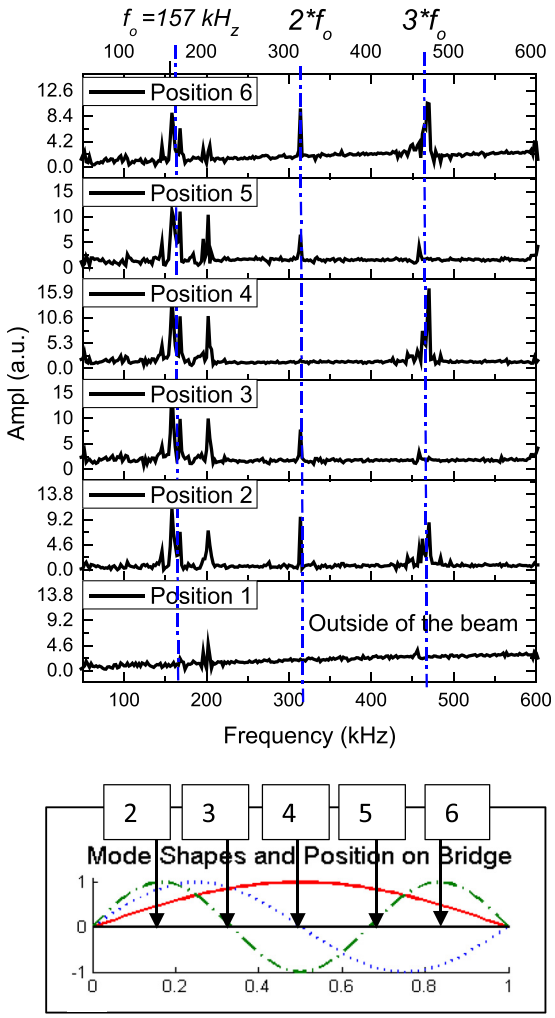

FIG. 2. (a) Resonance spectrum at zero field measured by LDV read out at different positions on the beam and (b) fundamental modes for corresponding positions (1–6) of the laser beam on the device.

$$f_r = \frac{\pi}{2L^2}\sqrt{\frac{Ewt^3}{12\rho}}, \tag{1}$$

where L, w, and t are the beam length, width, and thickness, E is Young's modulus, and ρ is the density. Evaluation of this equation with conventional material parameters for $Co_{68}Fe_{32}$ ($E = 170$ GPa, $\rho = 8370$ kg/m^3) and beam dimensions results in resonance frequencies on the order of less than 1 kHz. Our measurements show it is not unreasonable to assume each bridge as a one-dimensional string, which yields

$$f_r = \frac{1}{2L}\sqrt{\frac{\sigma}{\rho}}, \tag{2}$$

where σ is the uniaxial stress in the length direction. For a typical 1-mm long bridge with a resonance at ~130 kHz (Fig. 1), it is found that $\sigma = 580$ MPa, which is quite close to the yield value.[18]

As expected for a beam under high tensile stress, halving the length of the bridge to 0.5 mm led to a resonance frequency of approximately twice (256 kHz), which was confirmed by the fact that the frequency component was present in the FFT at all locations (Positions 2–6, Fig. 2(b)) along the

length of the bridge but not on the substrate. Additionally, for both lengths, harmonic frequencies were observed at two and three times that of the fundamental mode.

The low-field magnetic field dependence of the beam fundamental mode resonant frequency was measured with a position-sensitive detector and beam deflection implemented within a commercial atomic force microscope (AFM) (Asylum MFP-3D). Alternatively, as a control method, a transverse mode at zero field was continuously driven with the piezoelectric stack of a DI3100 AFM, loaded on the head as if it were a standard AFM tip. From the automated tuning program for tapping mode operation and the built-in laser and photodiode arrangement, the vibration frequency was swept from dc to 400 kHz. The laser was focused on a bridge, and the response was measured with the photodiode. Both techniques confirmed the frequencies measured with dynamic mode Zygo optical profilometer and the LDV impulse excitation. A magnetic field **H** of up to ~200 Oe was applied parallel to the beam axis. During application of field, the deflection amplitude and phase of the beam in response to a frequency-modulated driving voltage applied to an integrated piezoelectric stack were measured. In addition, the thermal noise power spectral density (in the absence of a driving force) was collected, with a spectral resolution of 1 Hz when collecting over a narrow range of frequencies shown in Fig. 3. Application of **H** perpendicular to the beam axis resulted in a change of f_r up to 10 kHz/T while there was practically no change for **H** || the beam axis.

High magnetic field dependence of resonance frequency was measured by LDV for magnetic field magnitude up to $\mu_0 H \sim 0.3$ T as shown in Fig. 4(b). At low field, f_r changes as a parabolic function of H for $\mu_0 H < 0.03$ T, followed by an approximately linear regime at fields between 0.03 and 0.1 T, and saturating above ~0.2 T. This is consistent with magnetization curve measured by VSM as shown in Fig. 4(a). In agreement with low-field scans, the effect is negligible for **H** applied along the beam axis; however, there is a marked shift when the **H** is applied normal to the beam as found at low field by the AFM technique.

By minimizing the free energy and solving for the stress, Eq. (2) yields that for fields which exceed that required for magnetic saturation

$$f_s = \frac{1}{2L}\sqrt{\frac{\sigma + (1+\upsilon)\lambda_s E}{\rho}}, \tag{3}$$

where υ is the Poisson ratio. Assuming $E = 170$ GPa and $\upsilon = 0.3$, λ_s is estimated to be 29 ppm. This value is in a good agreement with the literature values for magnetostriction of $Fe_{30}Co_{70}$ thin films (~30…70 ppm (Ref. 16)). Since the magnetostriction constant λ of CoFe is positive and the bridge is under substantial tensile stress, the magnetic easy axis is coincident with the beam axis. Thus, at zero field, the beam contains magnetic domains whose magnetization lies along the beam axis. If the field is directed along the beam, then the domains will change size but there will be no change in stress. However, if the field is normal to the beam axis, the domains will rotate. Unlike conventional magnetostrictive devices, the length does not change as it is fixed by the boundary conditions so the tensile stress in the bridge

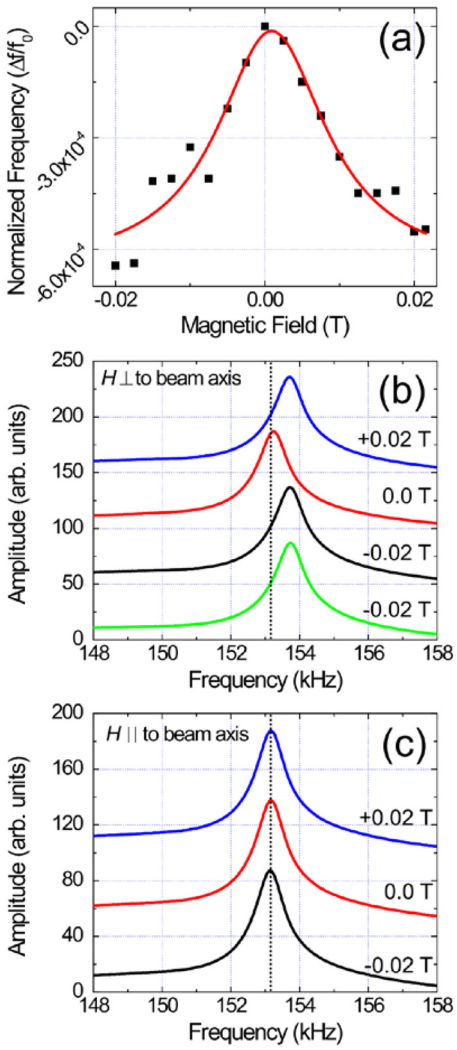

FIG. 3. (a) Variation in normalized fundamental bending-mode frequency with field applied perpendicular to the beam axis, and resonance peaks for different values of field applied (b) parallel to, and (c) perpendicular to beam axis.

increases, leading to higher resonance frequency, in accord with observations. Under such high tension, the stress anisotropy $K_\sigma \sim 3\lambda\sigma/2 \sim 20$ kJ/m^3 is expected to be larger than magnetocrystalline anisotropy and therefore the effect of frequency tuning by magnetic field is controlled by interplay between stress- and shape-induced anisotropy energies.

We notice that the equivalent noise for detection principle based on magnetic field dependence of resonant frequency could be significantly lowered by increasing the intrinsic sensor sensitivity. The sensitivity $(1/\mu_0)df/dH$ is determined in the vicinity of maximum slope $f(H)$ (Fig. 4(b)) of the magnetic field dependence of resonant frequency which is maximum at the operating magnetic field bias $\mu_0 H_0 \sim 0.025$ T. As it can be observed from Fig. 4(b), the 1-mm beam sensitivity is ~10 kHz/T, which is at least 2000× better as compared to macroscopic ME sensors.[17] Based on experimental results and the low magnetostriction factor, we assume that the intrinsic magnetic noise b_n (T/$\sqrt{}$Hz) of the bridge is ultimately determined by the spectral density of the white noise stress level σ_n (Pa/$\sqrt{}$Hz) in the vicinity of the resonant frequency f_r and given by

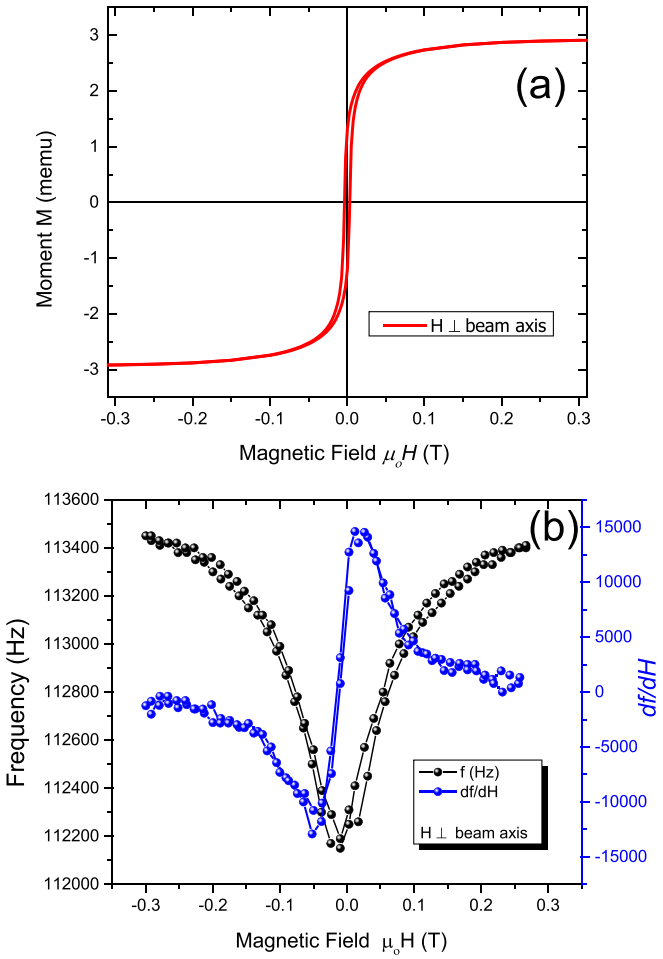

FIG. 4. (a) *M-H* curve of the FeCo devices array for two orientation of the beam. (b) Large field frequency shift for 1 mm bridge measured by LDV. Also shown first derivative of the field frequency dependence *df/dH*. The results clearly show maximum sensitivity near $\mu_0 H \sim 0.025$ T corresponding.

$$b_n = \left|\mu_0 \left(\frac{dH}{df_r}\right)\left(\frac{df_r}{d\sigma}\right)\right|\sigma_n. \tag{4}$$

By Eq. (2), $df_r/d\sigma = f_r/2\sigma$. From the Nyquist model[19,20]

$$\sigma_n \sim \frac{2}{A}\sqrt{\frac{2\pi k_B T f_r m}{Q}}, \tag{5}$$

where A *is* the cross-sectional area, k_B is the Boltzmann constant, T is the absolute temperature, m is the mass, and Q is the mechanical quality factor. This yields

$$b_n \sim \frac{\mu_0}{2}\left(\frac{dH}{df_r}\right)\sqrt{\frac{2\pi k_B T f_r}{QV\sigma}} = \frac{\mu_0}{2}\left(\frac{dH}{df_r}\right)\sqrt{\frac{\pi k_B T}{QVL\sigma^{1/2}\rho^{1/2}}}, \tag{6}$$

where V is the volume of the device. Equation (6) predicts $b_n(f) \sim 100$ pT/$\sqrt{}$Hz at room temperature, if the sensor sensitivity and the equivalent frequency dynamic range of the setup are high enough to neglect its equivalent magnetic noise.

In this Letter, we have described the fabrication and characterization of free-standing CoFe thin film bridges and demonstrated the change in resonance frequency of first bending mode as a function of magnetic field applied predominantly perpendicularly to the length of the bridges due to stress-induced magnetic anisotropy. We have studied this effect of magnetic field tuning of the resonant frequency that could be attributed to a competition between stress-induced and shape-induced anisotropy energies on magnetic hysteresis loops, and domain configurations. Magnetic field sensitivity of these high frequency mesoscopic devices at least of several orders of magnitude improved as compared to previously reported large scale ME composites making them promising candidate for near dc magnetic field sensors. It is believed these devices could be used as the basis for a fully integrated ME devices by adding a layer of ferroelectric thin film on top of the existing CoFe film to generate an electrical ME voltage read-out.[12,21] Fabricating such a device and characterizing the effectiveness of the magnetoelectric coupling will be the next phase of this research.

The authors would like to acknowledge the Office of Naval Research and the University Laboratory Internship (ULI) program for support of this work. Thanks also to Dr. Jain at the University of Connecticut, who provided use of his laboratory to complete the sample fabrication.

[1]J. van Suchtelen, Philips Res. Rep. **27**, 28 (1972).
[2]T. Nan, Y. Hui, M. Rinaldi, and N. X. Sun, Nat. Sci. Rep. **3**, 1985 (2013).
[3]T. Wu and G. P. Carman, J. Appl. Phys. **112**, 073915 (2012).
[4]J. Lou, D. Reed, M. Liu, and N. X. Sun, Appl. Phys. Lett. **94**, 112508 (2009).
[5]V. Castel and C. Broseau, Appl. Phys. Lett. **92**, 233110 (2008).
[6]P. Li, Y. Wen, P. Liu, X. Li, and C. Jia, Sens. Actuators, A **157**, 100 (2010).
[7]C. L. Zhang, J. S. Yang, and W. Q. Chen, Appl. Phys. Lett. **95**, 013511 (2009).
[8]S. Priya, J. Ryu, C. S. Park, J. Oliver, J. J. Choi, and D. S. Park, Sensors **9**(8), 6362 (2009).
[9]Z. Zhang, X. Z. Dai, and Y. Wang, Adv. Mater. Res. **722**, 75 (2013).
[10]Y. Wang, D. Gray, D. Berry, J. Gao, M. Li, J. Li, and D. Viehland, Adv. Mater. **23**, 4111 (2011).
[11]S. Dong, J. F. Li, and D. Viehland, Appl. Phys. Lett. **85**, 2307 (2004).
[12]T.-D. Onuta, Y. Wang, C. J. Long, and I. Takeuchi, Appl. Phys. Lett. **99**, 203506 (2011).
[13]M. S. Keshner, Proc. IEEE **70**, 212 (1982).
[14]A. S. Edelstein and G. A. Fischer, J. Appl. Phys. **91**, 7795 (2002).
[15]D. Niarchos, Sens. Actuators, A **109**, 166 (2003).
[16]D. Hunter, W. Osborn, K. Weng, N. Kazantseva, J. Hattrick-Simpers, R. Suchoski, R. Takahashi, M. L. Young, A. Mehta, L. A. Bendersky, S. E. Lofland, M. Wuttig, and I. Takeuchi, Nat. Commun. **2**, 518 (2011).
[17]J. Kiser, P. Finkel, J. Gao, C. Dolabdjian, J. Li, and D. Viehland, Appl. Phys. Lett. **102**, 042909 (2013).
[18]X. M. Cheng, X. K. Zhang, D. Z. Zhang, S. H. Lee, A. Duckham, T. P. Weihs, R. C. Cammarata, J. Q. Xiao, and C. L. Chien, J. Appl. Phys. **93**, 7121 (2003).
[19]T. B. Gabrielson, IEEE Trans. Electron Devices **40**, 903 (1993).
[20]S. A. Cavill, D. E. Parkes, J. Miguel, S. S. Shesi, K. W. Edmonds, and R. P. Campi, Appl. Phys. Lett. **102**, 032405 (2013).
[21]S. Marauska, R. Jahns, C. Kirchhof, M. Claus, E. Quandt, R. Knochel, and B. Wagner, Sens. Actuators, A **189**, 321–327 (2013).